J|A|C|S COMMUNICATIONS

Tracing the Reaction Steps Involving Oxygen and IR Observable Species in Ethanol Photocatalytic Oxidation on TiO_2

Felipe Guzman and Steven S. C. Chuang*

The University of Akron, Department of Chemical and Biomolecular Engineering, 200 East Buchtel Commons, Akron, Ohio 44325-3906

Received September 5, 2009; E-mail: schuang@uakron.edu

Photocatalytic oxidation of organics on TiO_2 has long been shown to occur via generation of light-induced charge carriers (i.e., electron/hole pairs) and charge transfer reactions of electrons and holes to species adsorbed on the surface. Transient spectroscopic studies have demonstrated that charge carrier generation and charge transfer reactions occur in time scales of femtoseconds and nanoseconds,[1] whereas the overall conversion of organics to CO_2 and H_2O occur in a time scale of minutes to hours. The factors governing the slow conversion of reactants and the rate-determining steps in photocatalytic reactions have seldom been studied.[2] We have identified the rate-determining step in the photocatalytic oxidation of ethanol by an in situ infrared (IR) spectroscopy coupled with mass spectrometry method. Ethanol was selected as a model molecule for tracing the reaction pathways because it produces IR-observable adsorbed species and possesses the ability to displace adsorbed H_2O, slowing down electron and hole recombination.

The reaction steps involving O_2 and IR-observable species were studied by illuminating adsorbed ethanol on TiO_2 (P 25, Degussa) with UV light (25 mW/cm^2) and dosing small amounts of O_2 (i.e., pulsing 10−500 μL of O_2) into a 15 cm^3/min He stream flowing through the DRIFT cell. The evolution of gaseous species was quantified with a mass spectrometer (MS, Pfeiffer Omnistar) connected to the outlet of the DRIFT cell.

The top spectrum in Figure 1A (i.e., spectrum at 0 min) shows ethanol adsorbed as ethoxy ($CH_3CH_2O_{ad}$) and molecularly adsorbed ethanol ($CH_3CH_2OH_{ad}$), giving the increased intensity of the C−H bands at 2971, 2931, and 2870 cm^{-1}. The formation of $CH_3CH_2O_{ad}$ can be distinguished by the intense ν(C−O) band at 1147 cm^{-1} and the low intensity ratio of δ(OH)/δ(CH). The appearance of the ethanol bands was accompanied by the decreased (i.e., negative) hydroxyl bands at 3632 and 3692 cm^{-1} and the HOH bending at 1625 cm^{-1}, indicating that adsorption of ethanol consumed the hydroxyl groups and displaced H_2O from the TiO_2 surface. The initial surface coverage was determined to be 820 μmol/g TiO_2 for adsorbed ethanol/ethoxy and 980 μmol/g TiO_2 for H_2O_{ad}. The spectrum at 0.6 min in Figure 1A shows that UV illumination caused the decrease in the intensity of the ethanol C−H bands and the rise of an IR structureless background absorbance in the 3000−1000 cm^{-1} range (i.e., background shift), attributed to photogenerated electrons accumulating on the conduction band.[3−5] The absence of variation in the IR intensity of the H_2O and OH bands during this period indicates that the intensity decrease of the C−H bands was the result of the reaction of $CH_3CH_2O_{ad}$/$CH_3CH_2OH_{ad}$ with h^+ (i.e., holes), allowing accumulation of the photogenerated electrons giving the intense background shift.[6]

Pulsing O_2 on ethanol adsorbed on the TiO_2 caused a decrease in the extent of the background shift intensity, as shown by the spectrum at 30 min in Figure 1A, indicating that O_2 directly reacted with photogenerated electrons.[4] Subsequent O_2 pulses (e.g., spectrum at 76 min) produced similar changes on the background shift intensity accompanied by the formation of adsorbed acetate ($CH_3COO^-_{ad}$) at 1542 and 1441 cm^{-1}, adsorbed H_2O, and CO_2.[6,7]

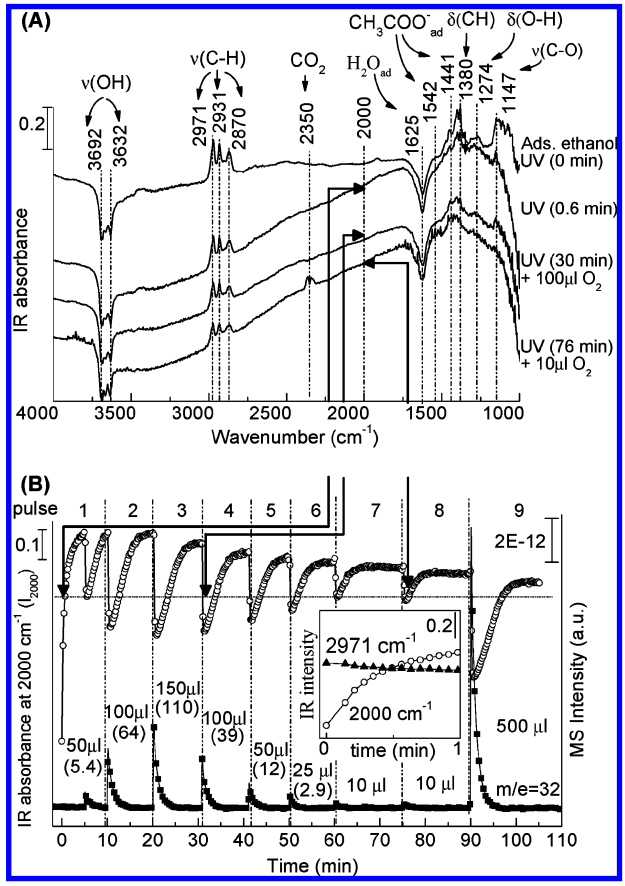

Figure 1. (A) IR spectra recorded during photocatalytic oxidation of adsorbed (Ads.) ethanol with O_2 pulses. Absorbance is obtained by Abs. = $-\log(I/I_0)$ where I and I_0 are the single beam spectra taken during and prior to ethanol adsorption, respectively. The negative bands indicates the decrease in the IR intensity (I) with respect to I_0. (B) Variation of the IR intensity at 2000 cm^{-1}, MS profile of O_2 concentration, and volume of O_2 pulsed and adsorbed; the latter shown in μL in parentheses.

The reaction process for producing these IR-observable species can be described by Scheme 1.

Scheme 1

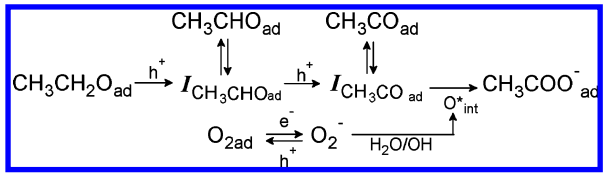

10.1021/ja907256x

The oxygen adsorption step and its interaction with photogenerated electrons ($O_{2ad} + e^- \rightarrow O_2^-$) can be further examined by comparing the intensity of the background shift, measured as the IR absorbance intensity at 2000 cm^{-1} (I_{2000}) and the O_2 concentration profile, as presented in Figure 1B. I_{2000} has been used to quantify the extent of the background shift due to the absence of overlapping bands.[4] Expanding the initial IR intensities versus time in the inset of Figure 1B shows the rapid rise in I_{2000}, accompanied by the gradual decay of the C−H intensity, highlighting the fact that the process of electron and hole generation is significantly faster than the hole-abstracting reaction ($CH_3CH_2O_{ad} + h^+ \rightarrow \boldsymbol{I}_{CH_3CHO_{ad}}$). $\boldsymbol{I}_{CH_3CHO_{ad}}$ would be a common intermediate for the formation of $CH_3COO^-_{ad}$, CH_3CHO_{ad}, and CH_3CO_{ad}. The presence of such an intermediate can be inferred from the observation of the evolution of $CH_3COO^-_{ad}$ at 1542 and 1441 cm^{-1}, which preceded that of CH_3CHO_{ad} at 1718 cm^{-1}, and CH_3CO_{ad} at 1650 cm^{-1},[8] as shown in Figure 2.

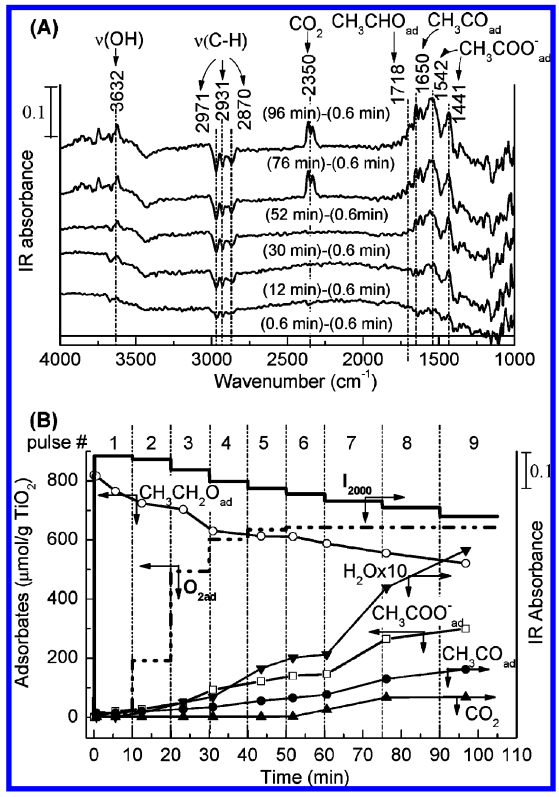

Figure 2. (A) Difference IR spectra of adsorbed species and CO_2. (B) Variation of the coverage of adsorbed species as a function of UV illumination time. The dotted line represents the cummulative coverage of O_{2ad}, and the continuous black line the resulting IR intensity at 2000 cm^{-1} (I_{2000}) after each O_2 addition.

Each O_2 pulse caused the adsorption of O_2 and the sudden decrease in I_{2000} followed by a gradual recovery to nearly its initial intensity. Since the TiO_2 temperature and the irradiation intensity are constant, the rate of photoelectron and hole generation is expected to be constant. Thus, the decrease in the extent of the I_{2000} recovery can be attributed to (i) the reaction of O_2 and electrons[9] ($O_2 + e^- \rightarrow O_2^-$) and (ii) an increase in the rate of electron and hole recombination. The O_2^- produced can react with OH groups or H_2O on the TiO_2 surface to form oxygen reactive intermediates (O^*_{int}) such as hydroxyl radicals (•OH)[1]. Although we do not have direct evidence of the formation of these oxygen intermediates, their formation has been well established.[10] The O^*_{int} can further react with $\boldsymbol{I}_{CH_3CHO_{ad}}$ or CH_3CO_{ad} to produce $CH_3COO^-_{ad}$ ($CH_3CO_{ad} + O^*_{int} \rightarrow CH_3COO^-_{ad}$) and ultimately CO_2, through the Koble reaction.[11] The specific nature of the O^*_{int} requires further Electron Spin Resonance (ESR) studies and correlating the ESR signal of O* with the infrared intensity of CH_3CO_{ad} and $CH_3COO^-_{ad}$. The formation of $CH_3COO^-_{ad}$ and CH_3CO_{ad} can be unambiguously determined by the difference IR spectra in Figure 2A, which were obtained by subtracting spectra exhibiting the same I_{2000} intensity. The IR intensities of $CH_3COO^-_{ad}$, the major intermediate of the reaction, were further calibrated with those of adsorbed ethanol and CO_2 to convert them to the quantities shown in Figure 2B (details presented in Supporting Information).

Figure 2B shows formation of $CH_3COO^-_{ad}$ preceded that of CH_3CHO_{ad}, suggesting the abundance of h^+ and O^*_{int} for reacting with $\boldsymbol{I}_{CH_3CHO_{ad}}$. In turn, CH_3CHO_{ad} can only be formed when O_2 adsorption is limited, as shown in the ninth pulse. The O_{2ad} from the first three pulses, which corresponds to 494 μmol/g TiO_2, caused a 5.3% decrease of I_{2000} with the formation of negligible CO_2/H_2O and 31% of the final acetate coverage. The subsequent 3 pulses reduced 9.3% of I_{2000} and produced additional 17.6% of the final acetate coverage. This observation indicates that (i) the initial O_{2ad} fills those TiO_2 surface sites which do not have a significant influence on the electron and hole recombination rate and (ii) sufficient coverage of O_2^- is needed to increase the rate of electron and hole recombination and initiate formation of $CH_3COO^-_{ad}$ and H_2O. Further O_2 additions did not increase the O_{2ad} coverage, but resulted in a significant increase in the formation of CH_3CO_{ad}, CO_2, and H_2O with a slight decrease in I_{2000}. As the coverage of O_{2ad} approached 640 μmol/g TiO_2 and the accumulation of acetate reached 300 μmol/g TiO_2, the addition of a large O_2 pulse at 90 min produced little changes in O_{2ad} and formation of $CH_3COO^-_{ad}$ and CO_2, indicating that the oxygen adsorption step is a rate-limiting step. These observations for pulsing O_2 over adsorbed ethanol on TiO_2 were found to be consistent with the results of pulsing ethanol/O_2 (1/1 molar ratio) on TiO_2 without preadsorbed ethanol, as described in the Supporting Information. In conclusion, IR coupled with the MS method showed that the oxygen adsorption step controls the overall reaction process; this step is further slowed down by the presence of the stable acetate on the TiO_2 surface. The effective removal of carboxylate species from the catalyst holds the key to accelerating the rate of photocatalytic oxidation of organics. This study bridges the gap between the results of nanosecond and millisecond time transient absorption studies and that of minute scale photocatalytic oxidation studies.

Acknowledgment. This work was partially supported by the U.S. Department of Energy (Grant DE-FG26-01NT41294) and FirstEnergy Corp.

Supporting Information Available: Additional experiments. This material is available free of charge via the Internet at http://pubs.acs.org.

References

(1) Hoffmann, M. R.; Martin, S. T.; Choi, W.; Bahnemann, D. W. *Chem. Rev.* **1995**, *95*, 69–96.
(2) Morris, N. D.; Suzuki, M.; Mallouk, T. E. *J. Phys. Chem. A* **2004**, *108*, 9115–9119.
(3) Szczepankiewicz, S. H.; Colussi, A. J.; Hoffmann, M. R. *J. Phys. Chem. B* **2000**, *104*, 9842–9850.
(4) Berger, T.; Sterrer, M.; Diwald, O.; Knoezinger, E.; Panayotov, D.; Thompson, T. L.; Yates, J. T., Jr. *J. Phys. Chem. B* **2005**, *109*, 6061–6068.
(5) Yamakata, A.; Ishibashi, T.-A.; Onishi, H. *J. Mol. Catal. A: Chem.* **2003**, *199*, 85–94.
(6) Chuang, S. S. C.; Guzman, F. *Top. Catal.* **2009**, *52*, 1448–1458.
(7) Muggli, D. S.; Lowery, K. H.; Falconer, J. L. *J. Catal.* **1998**, *180*, 111–122.
(8) Chuang, S. S. C.; Pien, S. I. *J. Mol. Catal.* **1989**, *55*, 12–22.
(9) Henderson, M. A.; Epling, W. S.; Peden, C. H. F.; Perkins, C. L. *J. Phys. Chem. B* **2003**, *107*, 534–545.
(10) Anpo, M.; Shima, T.; Kubokawa, Y. *Chem. Lett.* **1985**, 1799–802.
(11) Kraeutler, B.; Bard, A. J. *J. Am. Chem. Soc.* **1978**, *100*, 2239–40.

JA907256X